Cell PRESS
Neuron
Report

The Endocannabinoid 2-Arachidonoylglycerol Produced by Diacylglycerol Lipase α Mediates Retrograde Suppression of Synaptic Transmission

Asami Tanimura,[1,6] Maya Yamazaki,[3,6] Yuki Hashimotodani,[1] Motokazu Uchigashima,[4] Shinya Kawata,[1] Manabu Abe,[3] Yoshihiro Kita,[2] Kouichi Hashimoto,[1,5] Takao Shimizu,[2] Masahiko Watanabe,[4] Kenji Sakimura,[3] and Masanobu Kano[1,*]
[1]Department of Neurophysiology
[2]Department of Biochemistry and Molecular Biology
Graduate School of Medicine, University of Tokyo, Tokyo 113-0033, Japan
[3]Department of Cellular Neurobiology, Brain Research Institute, Niigata University, Niigata 951-8585, Japan
[4]Department of Anatomy, Hokkaido University School of Medicine, Sapporo 060-8638, Japan
[5]CREST, PRESTO, Japan Science and Technology Agency, Saitama 332-0012, Japan
[6]These authors contributed equally to this work
*Correspondence: mkano-tky@m.u-tokyo.ac.jp
DOI 10.1016/j.neuron.2010.01.021

SUMMARY

Endocannabinoids are released from postsynaptic neurons and cause retrograde suppression of synaptic transmission. Anandamide and 2-arachidonoylglycerol (2-AG) are regarded as two major endocannabinoids. To determine to what extent 2-AG contributes to retrograde signaling, we generated and analyzed mutant mice lacking either of the two 2-AG synthesizing enzymes diacylglycerol lipase α (DGLα) and β (DGLβ). We found that endocannabinoid-mediated retrograde synaptic suppression was totally absent in the cerebellum, hippocampus, and striatum of DGLα knockout mice, whereas the retrograde suppression was intact in DGLβ knockout brains. The basal 2-AG content was markedly reduced and stimulus-induced elevation of 2-AG was absent in DGLα knockout brains, whereas the 2-AG content was normal in DGLβ knockout brains. Morphology of the brain and expression of molecules required for 2-AG production other than DGLs were normal in the two knockout mice. We conclude that 2-AG produced by DGLα, but not by DGLβ, mediates retrograde suppression at central synapses.

INTRODUCTION

Marijuana exerts psychomotor actions through cannabinoid CB_1 receptors that are widely distributed throughout the mammalian central nervous system (CNS). Their endogenous ligands (endocannabinoids) function as a retrograde messenger at central synapses and contribute to both short-term and long-term forms of synaptic modulation (Chevaleyre et al., 2006; Heifets and Castillo, 2009; Kano et al., 2009). Endocannabinoid release is triggered by strong depolarization of postsynaptic neurons and the resultant elevation of Ca^{2+} concentration (Ca^{2+}-driven endocannabinoid release [ER]) (Kreitzer and Regehr, 2001; Ohno-Shosaku et al., 2001; Wilson and Nicoll, 2001), strong activation of $G_{q/11}$-coupled receptors at basal intracellular Ca^{2+} level (basal receptor-driven endocannabinoid release [RER]) (Maejima et al., 2001), or simultaneous Ca^{2+} elevation and $G_{q/11}$-coupled receptor activation (Ca^{2+}-assisted RER) (Kim et al., 2002; Ohno-Shosaku et al., 2002a; Varma et al., 2001). Anandamide (Devane et al., 1992) and 2-arachidonoylglycerol (2-AG) (Mechoulam et al., 1995; Sugiura et al., 1995) have been regarded as two major endocannabinoids. Pharmacological data suggest that 2-AG functions as a retrograde messenger at synapses in various regions of the CNS (Kano et al., 2009). Inhibition of the 2-AG degrading enzyme monoacylglycerol lipase (MGL), but not the anandamide hydrolyzing enzyme fatty acid amidehydrolase (FAAH), increases the duration of depolarization-induced retrograde suppression (Hashimotodani et al., 2007c; Szabo et al., 2006). Inhibitors of the 2-AG-producing enzyme diacylglycerol lipase (DGL) have been reported to block RER (Galante and Diana, 2004; Haj-Dahmane and Shen, 2005; Jung et al., 2005; Maejima et al., 2005; Melis et al., 2004; Safo and Regehr, 2005). In contrast, there are a number of reports as to the effects of DGL inhibitors on Ca^{2+}-driven ER, but the results are controversial (Chevaleyre and Castillo, 2003; Hashimotodani et al., 2008; Safo and Regehr, 2005; Uchigashima et al., 2007). Moreover, DGL inhibitors have been reported to have side effects such as blocking CB_1 receptors (Palomäki et al., 2007).

Two closely related genes encoding DGL activity were cloned and named DGLα and DGLβ (Bisogno et al., 2003). Experiments with overexpression of DGLα (Bisogno et al., 2003) and those with pharmacological blockade or knockdown of endogenous DGLα/β by RNA interference (Bisogno et al., 2003; Jung et al., 2005) indicate that DGLα and/or DGLβ are major 2-AG synthesizing enzymes. To determine to what extent 2-AG mediates retrograde signaling and to clarify the relative contributions of DGLα and DGLβ in 2-AG biosynthesis, we generated mutant mouse lines lacking either of the two DGL isoforms. By analyzing these knockout mice, we demonstrate that 2-AG produced by DGLα, not by DGLβ, is a ubiquitous retrograde messenger at central synapses.

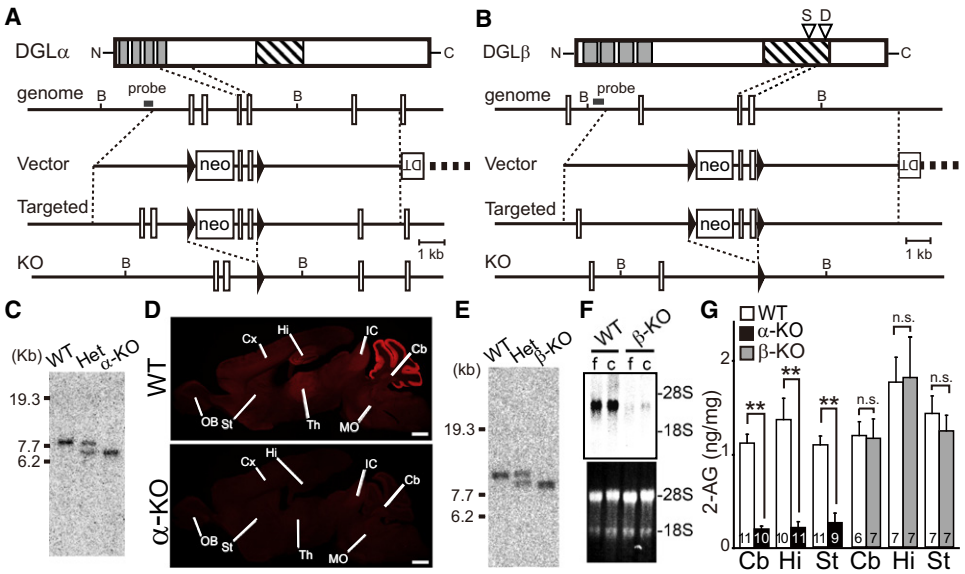

Figure 1. Generation of DGLα Knockout (α-KO) and DGLβ Knockout (β-KO) Mice

(A and B) Knockout strategy of *Dagla* (A) and *Daglb* (B) genes. Homologous recombination of the targeting plasmid resulted in insertion of the pgk-neo cassette (neo) and *loxP* sequences (filled triangles) into intron 2 and 4 of *Dagla* gene (A) or intron 9 and 11 of *Daglb* gene (B). After homologous recombination in ES cells followed by germline transmission (Targeted), the floxed mice were crossed with "Cre-deleter" mice. Exon 3 and 4 of *Dagla* gene (A) or exon 10 and 11 of *Daglb* gene (B) were deleted from germline (KO) together with the neo cassette. Four putative transmembrane domains and the serine lipase motif are indicated with gray and striped boxes, respectively. In (B), two putative catalytic triad serine and aspartate are indicated with inverted open triangles. B, BglII. (C) After Cre-mediated excision of exon 3 and 4 of *Dagla* gene, the BglII-digested 7.9 kb (WT) band shifted to 7 kb (α-KO). (D) Lack of DGLα immunofluorescence in α-KO brain. In WT mice, DGLα is expressed strongly in the cerebellar cortex and moderately in other brain regions, including the hippocampus and striatum. (E) After Cre-mediated excision of exon 10 and 11 of *Daglb* gene, the BglII-digested 8.9 kb (WT) band shifted to 7.95 kb (β-KO). (F) Lack of DGLβ transcript in β-KO mice. Northern blot analysis of total RNA samples from the forebrain (f) and cerebellum (c) of WT and β-KO mice (upper panel) and ethidium bromide staining of the corresponding agarose gel showing 28S and 18S ribosomal RNAs (lower panel) are shown. (G) Amount of 2-AG in block samples of cerebellum, striatum, and hippocampus from WT, α-KO, and β-KO mice. The number of samples is indicated within each column. **p< 0.01. See also Figure S1 and Table S1.

RESULTS

Generation of DGLα and DGLβ Knockout Mice

We generated null mutant mice lacking either DGLα or DGLβ by homologous recombination using the ES cell line RENKA, which we developed from the C57BL/6N strain (Mishina and Sakimura, 2007), followed by Cre-mediated deletion of the targeted genes (Figure 1 and Supplemental Experimental Procedures). DGLα knockout (α-KO) and DGLβ knockout (β-KO) mice were generated by disrupting exon 3 and 4 of *Dagla* gene (Figures 1A and 1C) and exon 10 and 11 of *Daglb* gene (Figures 1B and 1E), respectively. The resulting α-KO and β-KO mice are viable and appear normal with regard to their general appearances. Nissl staining of brains of α-KO and β-KO mice show that there are no perceptive abnormalities in the two knockout mice (Figure S1-1 available online). We verified that DGLα expression was normal in the brain of β-KO mice (Figure S2-2), whereas DGLα immunoreactivity was totally absent in α-KO mice (Figures 1D and S1-2). We confirmed that the DGLβ transcript was absent in the forebrain and cerebellum of β-KO mice (Figure 1F). We examined basic properties of synaptic transmission in acute slices of the cerebellum and striatum. Overall, kinetics of synaptic currents and paired-pulse ratio of α-KO and β-KO mice were not different from that of their wild-type (WT) littermates (Table S1 available online). We measured basal 2-AG contents in the cerebellum, striatum, and hippocampus, and found that the 2-AG contents were markedly decreased in α-KO mice (Figure 1G), whereas they were normal in the three brain regions of β-KO mice (Figure 1G). Therefore, the contribution of DGLα to 2-AG biosynthesis seems to be much greater than that of DGLβ in the CNS. In addition, basal contents of anandamide were decreased in the cerebellum and hippocampus of α-KO mice, whereas they were normal in β-KO mice (Figure S1-3).

Retrograde Suppression Is Deficient in the DGLα Knockout Cerebellum

We examined retrograde suppression of synaptic transmission by the three modes of endocannabinoid release in acute cerebellar slices. In WT mice, strong depolarization of Purkinje cells (PCs) caused Ca^{2+}-driven ER and readily induced transient suppression of excitatory synaptic transmission (depolarization-induced suppression of excitation [DSE]) from parallel fibers (PFs) (Figures 2A and 2B "PF-PC") and climbing fibers (CFs) (Figure 2B "CF-PC"), as well as transient suppression of synaptic transmission from inhibitory interneurons (INs) (depolarization-induced suppression of inhibition [DSI]) (Figure 2B "IN-PC"). DSE also occurred at PF to IN synapses following depolarization of INs (Figure 2B "PF-IN"). By marked contrast, DSE and DSI were totally absent in PCs and INs of α-KO mice (Figures 2A and 2B). We verified that Ca^{2+} transients in PCs

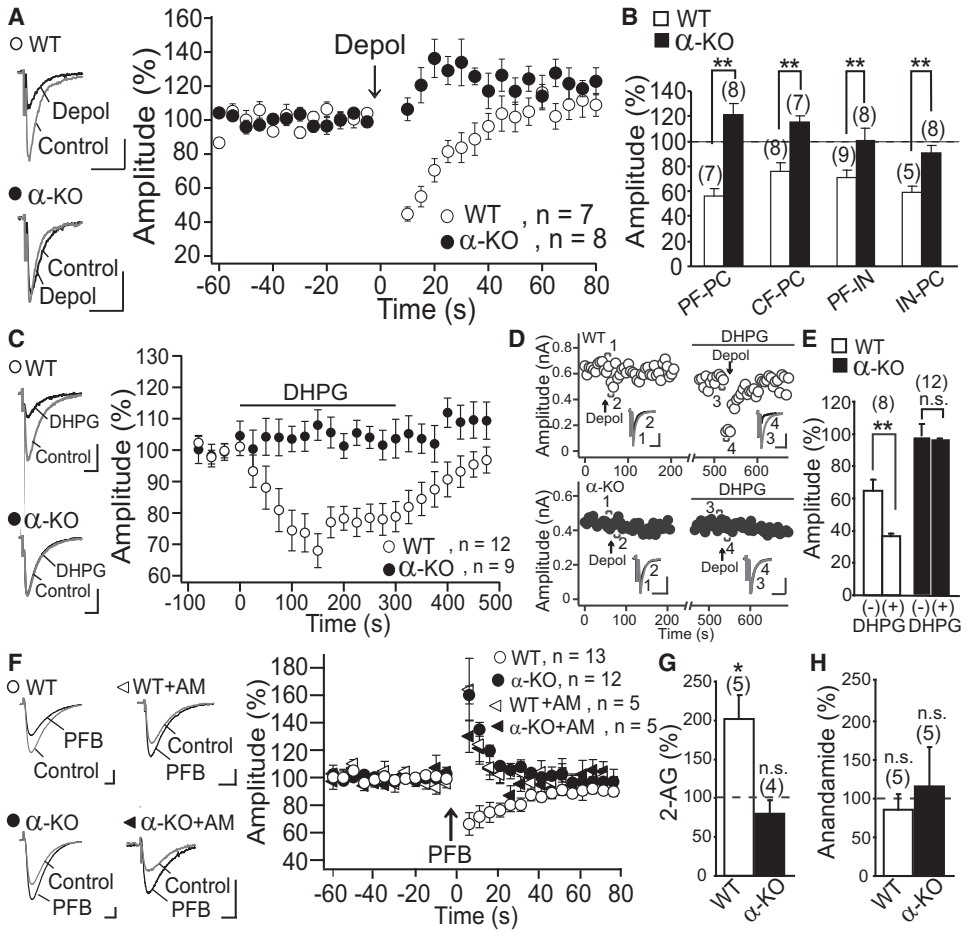

Figure 2. Endocannabinoid-Mediated Retrograde Suppression Is Absent in the Cerebellum of α-KO Mice

(A) Sample traces (left) and average time courses of PF-mediated EPSCs (right) from PCs of WT and α-KO mice before and after depolarization of PCs. (B) Summary bar graph showing the magnitudes of DSE at PF-PC, CF-PC, and PF-IN synapses, and those of DSI at IN-PC synapse. DSE at PF-PC and PF-IN synapses was induced by depolarizing postsynaptic neurons from −70 mV to 0 mV for 5 s. DSE at CF-PC synapses and DSI at IN-PC synapses was induced by a series of depolarizing pulses to PCs (5 [for DSE] and 10 [for DSI] depolarizing pulses from −70 mV to 0 mV with 100 ms duration at 1 Hz). (C) Sample traces (left) and average time courses of PF-EPSCs (right) before, during, and after bath application of DHPG (50 μM). (D and E) Representative experiment (D) and summary bar graph (E) showing enhancement of marginal DSE of CF-mediated EPSCs by weak depolarization (from −70 mV to 0 mV for 0.1 s) in the presence of a low dose (10 μM) of DHPG. (F) Sample traces (left) and average time courses of PF-EPSCs (right) before and after a burst of PF stimulation (PFB, 50 Hz, 50 pulses) recorded from PCs of WT mice and α-KO mice in the normal external solution or after treatment with AM251 (5 μM). (G and H) Summary bar graphs showing the percent changes in the 2-AG (G) and anandamide (H) levels of cerebellar slices from WT and α-KO mice after combined DHPG (100 μM) and high K^+ (20 mM) stimulation for 1 min. The number of cells for each experiment is indicated in parenthesis (B, E, G, and H). Calibration bars: 0.1 nA and 5 ms for (A), (C), and (F), and 0.2 nA and 5 ms for (D). *p < 0.05, **p < 0.01. See also Figure S2.

following DSE/DSI-inducing depolarization (Figures S2-1A through S2-1D), and cannabinoid sensitivities of PFs, CFs, and inhibitory synaptic terminals (Figure S2-1E), were normal in α-KO mice. These results indicate that the deficiency of DSE/DSI in α-KO cerebellum is not attributable to decreased Ca^{2+} transients, and that DGLα is indispensable for Ca^{2+}-driven ER in the cerebellum.

We then examined whether basal RER and Ca^{2+}-assisted RER were affected by deletion of DGLα. To test basal RER, we activated metabotropic glutamate receptor-subtype 1 (mGluR1), a $G_{q/11}$-coupled receptor strongly expressed in PCs, by bath application of its agonist, *R*,*S*-3,5-dihydroxyphenylglycine (DHPG). DHPG (50 μM) readily induced reversible suppression in WT mice, but this receptor-mediated suppression was totally absent in α-KO mice (Figure 2C). As for Ca^{2+}-assisted RER, marginal DSE at CF-PC synapses by weak depolarization of PCs was prominently enhanced when combined with subthreshold mGluR1 activation by a low dose of DHPG (10 μM) in WT mice (Maejima et al., 2005) (Figures 2D and 2E). Furthermore, a brief burst of PF stimulation caused Ca^{2+}-assisted RER by synaptically activated mGluR1 and transiently suppressed PF-PC transmission in WT mice (Brown et al., 2003; Maejima et al., 2005) (Figure 2F), which was reversed to a transient potentiation by the CB_1 antagonist AM251. Notably, both forms of Ca^{2+}-assisted RER were totally absent in α-KO mice (Figures 2D–2F). We verified that expression patterns and

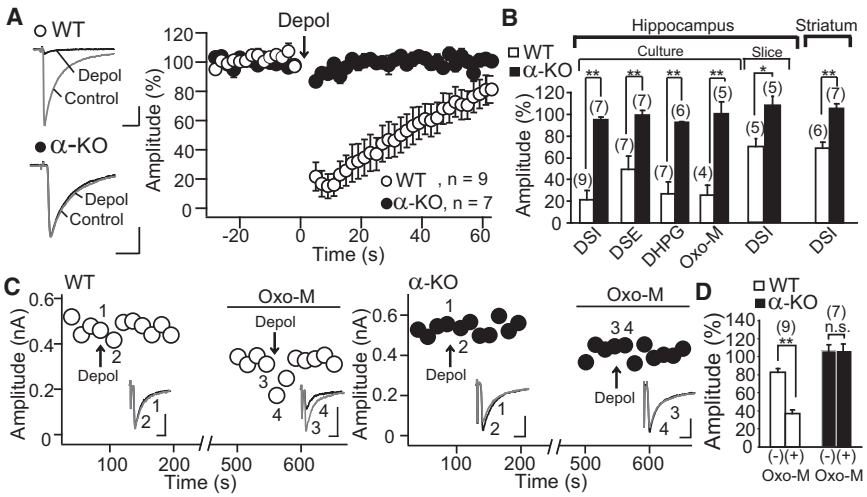

Figure 3. Endocannabinoid-Mediated Retrograde Suppression Is Absent in the Hippocampus and Striatum of α-KO Mice

(A) Sample traces (left) and average time courses of DSI (right) in cultured hippocampal neurons of WT and α-KO mice before and after depolarization (from −80 mV to 0 mV, for 5 s). (B) Summary bar graph showing the magnitudes of DSI, DSE, and retrograde suppression induced by DHPG and oxo-M in cultured hippocampal neurons, and those of DSI in hippocampal and striatal slices. (C and D) Representative experiments (C) and summary bar graph (D) showing the enhancement of marginal DSI (induced by depolarization from −70 mV to 0 mV for 0.1 s) by a low dose of oxo-M (0.5 μM) from medium spiny neurons of WT and α-KO striatum. The number of cells for each experiment is indicated in parenthesis (B and D). Calibration bars: 0.2 nA and 5 ms for (A) and (C). *p < 0.05, **p < 0.01. See also Figure S3.

protein levels of molecules involved in endocannabinid signaling (mGluR1, phospholipase C [PLC] β4, and CB_1) (Maejima et al., 2001, 2005; Yoshida et al., 2006) and mGluR1-mediated slow EPSCs in PCs (Batchelor and Garthwaite, 1997) were normal in the α-KO cerebellum (Figure S2-2). These results indicate that the lack of basal and Ca^{2+}-assisted RER in the cerebellum of α-KO mice is not attributable to changes in the expression of endocannabinoid signaling molecules. We also performed a biochemical experiment to measure stimulus-induced production of 2-AG in cerebellar slices. Combined application of DHPG (100 μM) and high K^+ (20 mM) solution elevated 2-AG level in WT mice (Figure 2G), which mimicked Ca^{2+}-driven RER in electrophysiological experiments (Maejima et al., 2005). In contrast, this combined stimulation caused no elevation of 2-AG in α-KO mice (Figure 2G). Importantly, the same stimulation caused no change in anandamide contents in cerebellar slices of WT and α-KO mice (Figure 2H). These results indicate that DGLα is indispensable for basal and Ca^{2+}-assisted RER in the cerebellum.

Retrograde Suppression Is Deficient in the Hippocampus and Striatum of DGLα Knockout Mice

We then examined endocannabinoid-mediated retrograde suppression in the hippocampus and striatum. In cultured hippocampal neurons, paired whole-cell recordings were performed and EPSCs and cannabinoid-sensitive unitary IPSCs were pharmacologically isolated. In WT mice, DSI (Figures 3A and 3B) and DSE (Figure 3B) were readily induced in the cannabinoid-sensitive IPSCs and EPSCs, respectively, following depolarization of the postsynaptic neuron from −80 mV to 0 mV for 5 s (Ohno-Shosaku et al., 2001, 2002b). The same depolarization protocols caused no appreciable suppression in IPSCs or EPSCs in hippocampal cultures prepared from α-KO mice (Figures 3A and 3B). In WT hippocampal neurons, activation of $G_{q/11}$-coupled receptors, mGluR5 by DHPG, and M_1/M_3 muscarinic acetylcholine receptors (mAChR-M_1/M_3) by oxotremorine-M (oxo-M) readily induced endocannabinoid-mediated retrograde suppression of IPSCs (Figure 3B). By contrast, these forms of receptor-mediated retrograde suppression were totally absent in α-KO mice (Figure 3B).

We also examined endocannabinoid-mediated retrograde suppression in hippocampal slices. Whole-cell recordings were made from CA1 pyramidal cells and IPSCs were evoked by stimulation in the stratum radiatum. DSI was readily induced by a series of depolarizing pulses (10 pulses of 100 ms duration, from −70 mV to 0 mV, repeated at 1 Hz) in WT mice, whereas DSI was totally absent in α-KO mice (Figure 3B). Bath application of DHPG (100 μM) caused long-term depression of IPSCs (I-LTD) in WT mice, as reported previously (Chevaleyre and Castillo, 2003). In contrast, DHPG failed to induce I-LTD in α-KO mice (Figure S3-1).

In striatal slices, whole-cell recordings were performed from medium spiny neurons and inhibitory inputs were stimulated around the recorded neurons (Narushima et al., 2006, 2007). In WT mice, DSI was readily elicited by a depolarizing pulse from −70 mV to 0 mV (5 s duration) (Figure 3B), and marginal DSI by a short-depolarization (a depolarizing pulse from −70 mV to 0 mV, 1 s duration) was significantly enhanced by a low dose (0.5 μM) of oxo-M (Figures 3C and 3D). By marked contrast, DSI (Figure 3B) and the enhancement of marginal DSI by a low dose of oxo-M (Figures 3C and 3D) were totally absent in α-KO mice.

We verified that cannabinoid sensitivities of IPSCs in hippocampal and striatal slices were normal in α-KO mice (Figure S3-2). Furthermore, we confirmed expression patterns and protein levels of molecules required for endocannabinoid signaling in the hippocampus and striatum (Hashimotodani et al., 2005; Uchigashima et al., 2007; Yoshida et al., 2006) including mGluR5, mAChR-M_1, PLCβ1, and CB_1, which were normal in α-KO mice (Figure S3-3). Thus, the lack of endocannabinoid-mediated retrograde suppression in their hippocampi and striati must result from the lack of DGLα.

Retrograde Suppression Is Normal in DGLβ Knockout Mice

We then examined whether DGLβ also contributes to retrograde signaling. Morphology of the brain (Figure S1-1) and expression patterns and protein levels of mGluR1/5, PLCβ1/4, mAChR-M_1, DGLα, and CB_1 were normal in β-KO mice (Figures S2-2 and S3-3).

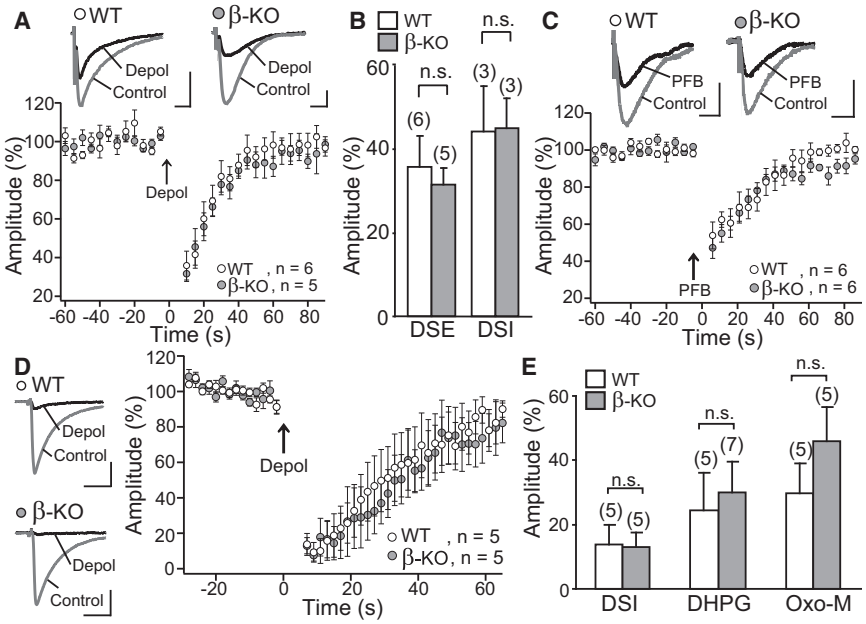

Figure 4. Endocannabinoid-Mediated Retrograde Suppression Is Intact in the Cerebellum and Hippocampus of β-KO Mice

(A) Sample traces (upper panel) and average time courses of PF-mediated EPSCs (lower panel) from PCs of WT and β-KO mice before and after depolarization of PCs. (B) Summary bar graph showing the magnitudes of DSE at PF-PC synapses and DSI at IN-PC synapses in the cerebellum. (C) Sample traces (upper panel) and average time courses of PF-EPSCs (lower panel) before and after a burst of PF stimulation (PFB, 50 Hz, 50 pulses) recorded from PCs of WT and β-KO mice. (D) Similar to (A) but for DSI in cultured hippocampal neurons. (E) Similar to (B) but for magnitudes of DSI, DHPG-induced suppression, and oxo-M-induced suppression in the hippocampus. The number of cells for each experiment is indicated in parenthesis (B and E). Calibration bars: 0.1 nA and 10 ms for (A) and (C), and 0.2 nA and 20 ms for (D). See also Figures S2-2 and S3-3.

We used the same experimental protocols to induce Ca^{2+}-driven ER, basal RER, or Ca^{2+}-assisted RER as used for WT and α-KO mice. We found that DSE at PF-PC synapses (Figures 4A and 4B) and DSI at IN-PC synapses (Figure 4B) in the cerebellum and DSI in cultured hippocampal neurons (Figures 4D and 4E) were normal in β-KO mice. Suppression of IPSCs induced by DHPG or oxo-M in hippocampal neurons was also normal (Figure 4E). Furthermore, suppression of PF-PC transmission by a PF burst was normal in β-KO mice (Figure 4C). Therefore, the three modes of endocannabinoid release, Ca^{2+}-driven ER, basal RER, and Ca^{2+}-assisted RER, are intact in β-KO mice.

Taken together, the present results strongly suggest that 2-AG produced by DGLα, and not by DGLβ, mediates retrograde signaling at central synapses.

DISCUSSION

We found that the three modes of endocannabinoid release and resultant retrograde suppression of synaptic transmission were totally absent in the cerebellum, hippocampus, and striatum of α-KO mice. The basal 2-AG content was markedly reduced in the three brain structures and the stimulus-induced elevation of 2-AG levels was absent in the cerebellum of α-KO mice. By contrast, endocannabinoid-mediated synaptic suppression and 2-AG content were normal in β-KO mice. Although the anandamide level was reduced in the cerebellum and hippocampus of α-KO mice, the extent of reduction was much smaller than 2-AG content. The cerebellum, hippocampus, and striatum have been most extensively studied for the mechanisms of endocannabinoid-mediated synaptic modulation. Many previous studies suggest that synapses in other brain regions share the same mechanisms of endocannabinoid release as those in the three brain structures (for review, see Chevaleyre et al., 2006; Hashimotodani et al., 2007b; Heifets and Castillo, 2009; Kano et al., 2009; Katona and Freund, 2008). Therefore, our results suggest that 2-AG produced by DGLα, not by DGLβ, likely accounts for most retrograde signaling at synapses throughout the CNS, although the possibility remains that anandamide or other endocannabinoids may be involved in other synapses.

Previous biochemical studies have revealed several pathways for 2-AG generation (Bisogno et al., 2005; Sugiura et al., 2006; Vandevoorde and Lambert, 2007). In the main pathway, PLCβ activated by $G_{q/11}$ hydrolyzes arachidonic acid-containing membrane phospholipid such as phosphatidylinositol, and produces arachidonic acid-containing diacylglycerol. Then, 2-AG is produced from the diacylglycerol by the action of DGLα and/or DGLβ. Besides this main cascade, alternative pathways for 2-AG generation are proposed, which include the sequential reactions by phospholipase A_1 (PLA_1) and lysoPI-specific PLC, the conversion from 2-arachidonoyl lysophosphatidic acid to 2-AG by phosphatase, and the formation from 2-arachidonoyl phosphatidic acid through 1-acyl-2-arachidonoylglycerol. However, the present results indicate that these alternative pathways are not involved in 2-AG generation for retrograde synaptic suppression.

Previous studies indicate that DGLα is expressed at postsynaptic sites of the neurons in various regions of the CNS (Katona et al., 2006; Lafourcade et al., 2007; Uchigashima et al., 2007; Yoshida et al., 2006). DGLα is most abundant around dendritic spines and is apposed closely to $G_{q/11}$-coupled receptors, $G_{q/11}$ protein α subunit, and PLCβ. Such a subcellular arrangement of molecules constitutes an anatomical basis for basal and Ca^{2+}-assisted RER (Hashimotodani et al., 2007a; Kano et al., 2009). The density of CB_1 expression in excitatory and inhibitory presynaptic terminals and the distances between the presynaptic terminals and the DGLα-rich postsynaptic structures are unique to each brain region (Katona et al., 1999; Kawamura et al., 2006). DGLα seems to be arranged such that the induction

threshold of 2-AG-mediated retrograde suppression of excitation and inhibition may be coordinated. In DGLα knockout mice, basal and Ca^{2+}-assisted RER was totally absent, although subcellular localizations of $G_{q/11}$-coupled receptors, PLCβ, and CB_1 were normal. Thus, the primary function of DGLα in central neurons seems to be the production of 2-AG that mediates retrograde synaptic suppression.

In contrast to DGLα, relatively little is known about subcellular localization of DGLβ at synapses. DGLβ was reported to be richly expressed in the PC soma but very low in dendrites (Suárez et al., 2008). This expression pattern is clearly different from that of DGLα (Yoshida et al., 2006). We expected that DSI of IN-PC synapses would have been smaller in β-KO mice if DGLβ in the PC soma had played a role in 2-AG production, because in this experiment we stimulated putative basket cell axons that form inhibitory synapses on the PC soma. However, our results demonstrate that DSI is normal in β-KO mice, suggesting that DGLβ has no contribution to retrograde synaptic suppression in PCs. In a recent study, DGLβ and DGLα were reported to be coexpressed in postsynaptic sites facing CB_1-rich excitatory terminals in the dorsal cochlear nucleus (Zhao et al., 2009). It is possible that DGLβ may participate in 2-AG production at synapses in limited brain regions.

Besides retrograde suppression at synapses, endocannabinoid signaling is reported to be involved in the regulation of cell proliferation, migration, differentiation, and survival during CNS development (Harkany et al., 2007). However, our morphological investigation revealed no apparent abnormality in gross anatomy of the α-KO and β-KO brains. Furthermore, basal synaptic transmission was normal in the cerebellum and striatum of α-KO and β-KO mice, indicating normal wiring and function of neural circuits. It is possible that the lack of DGLα or DGLβ may be compensated for by other signaling molecules during CNS development.

Behavioral studies have clarified the roles of the endocannabinoid system in various brain functions, including acquisition and/or extinction of certain forms of memory, regulation of anxious states, antidepressant effects, rewarding effects of some addictive compounds, promotion of appetite, relieving pain, and protecting neurons (for review, see Iversen, 2003; Kano et al., 2009). Many previous studies adopted pharmacological alteration of endocannabinoid signaling and/or local lesions to certain brain structures. However, such manipulations sometimes exert complex effects on animals' behaviors and thus the results are not necessarily consistent. In this respect, α-KO and β-KO mice will be useful tools for elucidating neural mechanisms underlying the behavioral effects of the endocannabinoid system. These mouse lines are also useful to clarify distinct roles of anandamide and 2-AG in various aspects of brain functions.

EXPERIMENTAL PROCEDURES

Generation of Knockout Mice

Experiments were conducted according to the guidelines of the animal welfare committees of the University of Tokyo, Hokkaido University, and Niigata University. α-KO and β-KO mice were generated by disrupting exon 3 and 4 of *Dagla* gene and exon 10 and 11 of *Daglb* gene, respectively, as illustrated in Figure 1 and detailed in the Supplemental Experimental Procedures.

Recordings from Cerebellar, Hippocampal, and Striatal Slices

Mice were decapitated following CO_2 anesthesia, and brains were rapidly removed and placed in chilled external solution (0°C–4°C) containing (in mM) 125 NaCl, 2.5 KCl, 2 $CaCl_2$, 1 $MgSO_4$, 1.25 NaH_2PO_4, 26 $NaHCO_3$, and 20 glucose, bubbled with 95% O_2 and 5% CO_2 (pH 7.4). For preparing hippocampal and striatal slices, NaCl was replaced with Choline-Cl. Parasagittal cerebellar slices (250 μm thick), transverse hippocampal slices (300 μm thick), or coronal forebrain slices containing the striatum (300 μm thick) were prepared by using a vibratome slicer (Leica, Germany).

Whole-cell recordings were made from visually identified PCs, CA1 pyramidal cells, or medium spiny neurons using an upright microscope (Olympus, Tokyo) at 32°C. Compositions of the pipette solutions and protocols of stimulation and recording are described in the Supplemental Experimental Procedures.

Paired Recordings from Cultured Hippocampal Neurons

Cultured hippocampal neurons were prepared from newborn mice as described (Ohno-Shosaku et al., 2001). The cultures were kept at 36°C in 5% CO_2 for 12–15 days before use. Each neuron of a pair was whole-cell voltage-clamped at room temperature. Compositions of the pipette and external solutions and protocols of stimulation and recording are described in the Supplemental Experimental Procedures.

Histology and Immunohistochemistry

Mice were fixed transcardially under deep pentobarbital anesthesia with 4% paraformaldehyde in 0.1 M phosphate buffer (pH 7.2), and brain sections (50 μm thickness) were prepared. Histology of the brain was examined with NeuroTrace 500/525 green fluorescent Nissl stain (Invitrogen, Carlsbad, CA). For immunohistochemistry, brain sections were incubated with 10% normal donkey serum for 20 min, primary antibodies overnight (for details, see the Supplemental Experimental Procedures; all primary antibodies were used at the final concentration of 1 μg/ml), and indocarbocyanine (Cy3)-labeled species-specific secondary antibodies for 2 hr at a dilution of 1:200 (Jackson ImmunoResearch, PA). Images were taken with a fluorescence microscope (AX-70; Olympus Japan) or with a confocal laser scanning microscope (FV1000; Olympus).

Quantification of 2-AG and Anandamide

For measuring basal 2-AG and anandamide contents in the cerebellum, striatum, and hippocampus, block samples were obtained from mice at 2–6 months of age, frozen immediately in liquid nitrogen, and stored at −80°C. Stimulus-induced production of 2-AG and anandamide by combined DHPG (100 μM) and KCl (20 mM) stimulation was measured in cerebellar slices (250 μm) prepared similarly to those used for electrophysiological experiments. Details of measurements of 2-AG and anandamide contents are described in the Supplemental Experimental Procedures.

Data Analysis

Data are represented as means ± SEM and the numbers of samples are indicated in figures. Statistical significance was assessed by Mann-Whitney U-test for two independent samples and Wilcoxon's signed rank test for paired samples.

SUPPLEMENTAL INFORMATION

Supplemental Information for this article includes three figures, one table, and Supplemental Experimental Procedures and can be found with this article online at doi:10.1016/j.neuron.2010.01.021.

ACKNOWLEDGMENTS

We thank T. Yoshida for helping with some experiments and R. Natsume for helping with the generation of knockout mice. This work has been supported by Grants-in-Aid for Scientific Research 17023021 (M.K.), 21220006 (M.K.), 18-08582 (Y.H.), 20-04030 (M.U.), and 17023001 (M.W.); the Strategic Research Program for Brain Sciences (Development of Biomarker Candidates

for Social Behavior); and the Global COE Program (Integrative Life Science Based on the Study of Biosignaling Mechanisms) from MEXT, Japan.

Accepted: January 16, 2010
Published: February 10, 2010

REFERENCES

Batchelor, A.M., and Garthwaite, J. (1997). Frequency detection and temporally dispersed synaptic signal association through a metabotropic glutamate receptor pathway. Nature *385*, 74–77.

Bisogno, T., Howell, F., Williams, G., Minassi, A., Cascio, M.G., Ligresti, A., Matias, I., Schiano-Moriello, A., Paul, P., Williams, E.J., et al. (2003). Cloning of the first *sn1*-DAG lipases points to the spatial and temporal regulation of endocannabinoid signaling in the brain. J. Cell Biol. *163*, 463–468.

Bisogno, T., Ligresti, A., and Di Marzo, V. (2005). The endocannabinoid signalling system: biochemical aspects. Pharmacol. Biochem. Behav. *81*, 224–238.

Brown, S.P., Brenowitz, S.D., and Regehr, W.G. (2003). Brief presynaptic bursts evoke synapse-specific retrograde inhibition mediated by endogenous cannabinoids. Nat. Neurosci. *6*, 1048–1057.

Chevaleyre, V., and Castillo, P.E. (2003). Heterosynaptic LTD of hippocampal GABAergic synapses: a novel role of endocannabinoids in regulating excitability. Neuron *38*, 461–472.

Chevaleyre, V., Takahashi, K.A., and Castillo, P.E. (2006). Endocannabinoid-mediated synaptic plasticity in the CNS. Annu. Rev. Neurosci. *29*, 37–76.

Devane, W.A., Hanus, L., Breuer, A., Pertwee, R.G., Stevenson, L.A., Griffin, G., Gibson, D., Mandelbaum, A., Etinger, A., and Mechoulam, R. (1992). Isolation and structure of a brain constituent that binds to the cannabinoid receptor. Science *258*, 1946–1949.

Galante, M., and Diana, M.A. (2004). Group I metabotropic glutamate receptors inhibit GABA release at interneuron-Purkinje cell synapses through endocannabinoid production. J. Neurosci. *24*, 4865–4874.

Haj-Dahmane, S., and Shen, R.Y. (2005). The wake-promoting peptide orexin-B inhibits glutamatergic transmission to dorsal raphe nucleus serotonin neurons through retrograde endocannabinoid signaling. J. Neurosci. *25*, 896–905.

Harkany, T., Guzmán, M., Galve-Roperh, I., Berghuis, P., Devi, L.A., and Mackie, K. (2007). The emerging functions of endocannabinoid signaling during CNS development. Trends Pharmacol. Sci. *28*, 83–92.

Hashimotodani, Y., Ohno-Shosaku, T., Tsubokawa, H., Ogata, H., Emoto, K., Maejima, T., Araishi, K., Shin, H.S., and Kano, M. (2005). Phospholipase Cβ serves as a coincidence detector through its Ca^{2+} dependency for triggering retrograde endocannabinoid signal. Neuron *45*, 257–268.

Hashimotodani, Y., Ohno-Shosaku, T., and Kano, M. (2007a). Ca^{2+}-assisted receptor-driven endocannabinoid release: mechanisms that associate presynaptic and postsynaptic activities. Curr. Opin. Neurobiol. *17*, 360–365.

Hashimotodani, Y., Ohno-Shosaku, T., and Kano, M. (2007b). Endocannabinoids and synaptic function in the CNS. Neuroscientist *13*, 127–137.

Hashimotodani, Y., Ohno-Shosaku, T., and Kano, M. (2007c). Presynaptic monoacylglycerol lipase activity determines basal endocannabinoid tone and terminates retrograde endocannabinoid signaling in the hippocampus. J. Neurosci. *27*, 1211–1219.

Hashimotodani, Y., Ohno-Shosaku, T., Maejima, T., Fukami, K., and Kano, M. (2008). Pharmacological evidence for the involvement of diacylglycerol lipase in depolarization-induced endocanabinoid release. Neuropharmacology *54*, 58–67.

Heifets, B.D., and Castillo, P.E. (2009). Endocannabinoid signaling and long-term synaptic plasticity. Annu. Rev. Physiol. *71*, 283–306.

Iversen, L. (2003). Cannabis and the brain. Brain *126*, 1252–1270.

Jung, K.M., Mangieri, R., Stapleton, C., Kim, J., Fegley, D., Wallace, M., Mackie, K., and Piomelli, D. (2005). Stimulation of endocannabinoid formation in brain slice cultures through activation of group I metabotropic glutamate receptors. Mol. Pharmacol. *68*, 1196–1202.

Kano, M., Ohno-Shosaku, T., Hashimotodani, Y., Uchigashima, M., and Watanabe, M. (2009). Endocannabinoid-mediated control of synaptic transmission. Physiol. Rev. *89*, 309–380.

Katona, I., and Freund, T.F. (2008). Endocannabinoid signaling as a synaptic circuit breaker in neurological disease. Nat. Med. *14*, 923–930.

Katona, I., Sperlágh, B., Sík, A., Käfalvi, A., Vizi, E.S., Mackie, K., and Freund, T.F. (1999). Presynaptically located CB_1 cannabinoid receptors regulate GABA release from axon terminals of specific hippocampal interneurons. J. Neurosci. *19*, 4544–4558.

Katona, I., Urbán, G.M., Wallace, M., Ledent, C., Jung, K.M., Piomelli, D., Mackie, K., and Freund, T.F. (2006). Molecular composition of the endocannabinoid system at glutamatergic synapses. J. Neurosci. *26*, 5628–5637.

Kawamura, Y., Fukaya, M., Maejima, T., Yoshida, T., Miura, E., Watanabe, M., Ohno-Shosaku, T., and Kano, M. (2006). The CB_1 cannabinoid receptor is the major cannabinoid receptor at excitatory presynaptic sites in the hippocampus and cerebellum. J. Neurosci. *26*, 2991–3001.

Kim, J., Isokawa, M., Ledent, C., and Alger, B.E. (2002). Activation of muscarinic acetylcholine receptors enhances the release of endogenous cannabinoids in the hippocampus. J. Neurosci. *22*, 10182–10191.

Kreitzer, A.C., and Regehr, W.G. (2001). Retrograde inhibition of presynaptic calcium influx by endogenous cannabinoids at excitatory synapses onto Purkinje cells. Neuron *29*, 717–727.

Lafourcade, M., Elezgarai, I., Mato, S., Bakiri, Y., Grandes, P., and Manzoni, O.J. (2007). Molecular components and functions of the endocannabinoid system in mouse prefrontal cortex. PLoS ONE *2*, e709.

Maejima, T., Hashimoto, K., Yoshida, T., Aiba, A., and Kano, M. (2001). Presynaptic inhibition caused by retrograde signal from metabotropic glutamate to cannabinoid receptors. Neuron *31*, 463–475.

Maejima, T., Oka, S., Hashimotodani, Y., Ohno-Shosaku, T., Aiba, A., Wu, D., Waku, K., Sugiura, T., and Kano, M. (2005). Synaptically driven endocannabinoid release requires Ca^{2+}-assisted metabotropic glutamate receptor subtype 1 to phospholipase Cβ4 signaling cascade in the cerebellum. J. Neurosci. *25*, 6826–6835.

Mechoulam, R., Ben-Shabat, S., Hanus, L., Ligumsky, M., Kaminski, N.E., Schatz, A.R., Gopher, A., Almog, S., Martin, B.R., Compton, D.R., et al. (1995). Identification of an endogenous 2-monoglyceride, present in canine gut, that binds to cannabinoid receptors. Biochem. Pharmacol. *50*, 83–90.

Melis, M., Pistis, M., Perra, S., Muntoni, A.L., Pillolla, G., and Gessa, G.L. (2004). Endocannabinoids mediate presynaptic inhibition of glutamatergic transmission in rat ventral tegmental area dopamine neurons through activation of CB_1 receptors. J. Neurosci. *24*, 53–62.

Mishina, M., and Sakimura, K. (2007). Conditional gene targeting on the pure C57BL/6 genetic background. Neurosci. Res. *58*, 105–112.

Narushima, M., Hashimoto, K., and Kano, M. (2006). Endocannabinoid-mediated short-term suppression of excitatory synaptic transmission to medium spiny neurons in the striatum. Neurosci. Res. *54*, 159–164.

Narushima, M., Uchigashima, M., Fukaya, M., Matsui, M., Manabe, T., Hashimoto, K., Watanabe, M., and Kano, M. (2007). Tonic enhancement of endocannabinoid-mediated retrograde suppression of inhibition by cholinergic interneuron activity in the striatum. J. Neurosci. *27*, 496–506.

Ohno-Shosaku, T., Maejima, T., and Kano, M. (2001). Endogenous cannabinoids mediate retrograde signals from depolarized postsynaptic neurons to presynaptic terminals. Neuron *29*, 729–738.

Ohno-Shosaku, T., Shosaku, J., Tsubokawa, H., and Kano, M. (2002a). Cooperative endocannabinoid production by neuronal depolarization and group I metabotropic glutamate receptor activation. Eur. J. Neurosci. *15*, 953–961.

Ohno-Shosaku, T., Tsubokawa, H., Mizushima, I., Yoneda, N., Zimmer, A., and Kano, M. (2002b). Presynaptic cannabinoid sensitivity is a major determinant of depolarization-induced retrograde suppression at hippocampal synapses. J. Neurosci. *22*, 3864–3872.

Palomäki, V.A., Lehtonen, M., Savinainen, J.R., and Laitinen, J.T. (2007). Visualization of 2-arachidonoylglycerol accumulation and cannabinoid CB_1

receptor activity in rat brain cryosections by functional autoradiography. J. Neurochem. *101*, 972–981.

Safo, P.K., and Regehr, W.G. (2005). Endocannabinoids control the induction of cerebellar LTD. Neuron *48*, 647–659.

Suárez, J., Bermúdez-Silva, F.J., Mackie, K., Ledent, C., Zimmer, A., Cravatt, B.F., and de Fonseca, F.R. (2008). Immunohistochemical description of the endogenous cannabinoid system in the rat cerebellum and functionally related nuclei. J. Comp. Neurol. *509*, 400–421.

Sugiura, T., Kondo, S., Sukagawa, A., Nakane, S., Shinoda, A., Itoh, K., Yamashita, A., and Waku, K. (1995). 2-Arachidonoylglycerol: a possible endogenous cannabinoid receptor ligand in brain. Biochem. Biophys. Res. Commun. *215*, 89–97.

Sugiura, T., Kishimoto, S., Oka, S., and Gokoh, M. (2006). Biochemistry, pharmacology and physiology of 2-arachidonoylglycerol, an endogenous cannabinoid receptor ligand. Prog. Lipid Res. *45*, 405–446.

Szabo, B., Urbanski, M.J., Bisogno, T., Di Marzo, V., Mendiguren, A., Baer, W.U., and Freiman, I. (2006). Depolarization-induced retrograde synaptic inhibition in the mouse cerebellar cortex is mediated by 2-arachidonoylglycerol. J. Physiol. *577*, 263–280.

Uchigashima, M., Narushima, M., Fukaya, M., Katona, I., Kano, M., and Watanabe, M. (2007). Subcellular arrangement of molecules for 2-arachidonoylglycerol-mediated retrograde signaling and its physiological contribution to synaptic modulation in the striatum. J. Neurosci. *27*, 3663–3676.

Vandevoorde, S., and Lambert, D.M. (2007). The multiple pathways of endocannabinoid metabolism: a zoom out. Chem. Biodivers. *4*, 1858–1881.

Varma, N., Carlson, G.C., Ledent, C., and Alger, B.E. (2001). Metabotropic glutamate receptors drive the endocannabinoid system in hippocampus. J. Neurosci. *21*, RC188.

Wilson, R.I., and Nicoll, R.A. (2001). Endogenous cannabinoids mediate retrograde signalling at hippocampal synapses. Nature *410*, 588–592.

Yoshida, T., Fukaya, M., Uchigashima, M., Miura, E., Kamiya, H., Kano, M., and Watanabe, M. (2006). Localization of diacylglycerol lipase-α around postsynaptic spine suggests close proximity between production site of an endocannabinoid, 2-arachidonoyl-glycerol, and presynaptic cannabinoid CB_1 receptor. J. Neurosci. *26*, 4740–4751.

Zhao, Y., Rubio, M.E., and Tzounopoulos, T. (2009). Distinct functional and anatomical architecture of the endocannabinoid system in the auditory brainstem. J. Neurophysiol. *101*, 2434–2446.